

# TRANS-DIMENSIONAL MONTE CARLO INVERSION OF SHORT PERIOD MAGNETOTELLURIC DATA FOR COVER THICKNESS ESTIMATION

**Ross C Brodie**

*Geoscience Australia  
GPO Box 378, Canberra, ACT, 2601  
Ross.C.Brodie@ga.gov.au*

**\*Wenping Jiang**

*Geoscience Australia  
GPO Box 378, Canberra, ACT, 2601  
Wenping.Jiang@ga.gov.au*

## SUMMARY

We have developed an algorithm and released open-source code for the 1D inversion of magnetotelluric data. The algorithm uses trans-dimensional Markov chain Monte Carlo techniques to solve for a probabilistic conductivity-depth model.

The inversion of each station employs multiple Markov Chains in parallel to generate an ensemble of millions of conductivity models that adequately fit the data given the assigned noise levels. The trans-dimensional aspect of the inversion means that the number of layers in the conductivity model is solved for rather than being predetermined and kept fixed. Each Markov chain increases and decrease the number of layers in the model and the depths of the interfaces as it samples.

Once the ensemble of models is generated, its statistics are analysed to assess the posterior probability distribution of the conductivity at any particular depth, as well as the number of layers and the depths of the interfaces. This stochastic approach gives a thorough exploration of model space and a more robust estimation of uncertainty than deterministic methods allow.

The method's application to cover thickness estimation is discussed with synthetic and real examples. Inversion of complex impedance tensor and also derived apparent resistivity/phase data are both demonstrated. It is found that the more pronounced layer boundaries allow more straightforward interpretation of cover thickness than that from deterministic smooth model inversions. It is concluded that thickness estimates compare favourably with borehole stratigraphic logs in most cases, and that the method is a useful addition to a range of cover thickness estimation tools.

**Key words:** Magnetotelluric, inversion, Monte Carlo, trans-dimensional.

## INTRODUCTION

Conventional methods for 1D inversion of magnetotelluric data are usually based on deterministic optimization techniques (Constable *et al.*, 1987). The solution is a single model, which fits the data within the assigned noise levels and conforms as closely as possible to the constraints imposed by some form of regularization. (Brodie and Sambridge, 2012) pointed out that due to non-uniqueness and data errors, the single model is just one of an infinite suite of models that could possibly fit the data within the noise levels. On its own, the single solution provides no information about the non-uniqueness or uncertainty in the solution. This lack of uncertainty information is recognized as a drawback of single-solution deterministic inversions. Some methods make use of the posterior model covariance matrix to estimate model parameter uncertainties. However, strictly speaking, such estimates are accurate only for linear problems and they cannot take account of the non-linearity or non-uniqueness of the electromagnetic inverse problem. They also often reflect the particular choice of regularization parameters.

To tackle the problem of non-uniqueness and uncertainty we present a trans-dimensional (often called reversible jump) Markov Chain Monte Carlo method to perform 1D magnetotelluric inversion via Bayesian inference. The algorithm provides not only a best fit model, but also a wealth of information about the uncertainty and non-uniqueness of the problem. The trans-dimensional aspect of the algorithm allows the number of layers in the resistivity model to be a parameter to be solved for in the inversion itself, meaning the number of layers does not need to be fixed in advance.

Transdimensional inversion has gained increasing traction in geophysics in the last decade, having being applied to resistivity data (Malinverno, 2002), seismic tomography and receiver function data (Bodin and Sambridge, 2009; Bodin *et al.*, 2012), airborne electromagnetics data (Minsley, 2011; Brodie and Sambridge, 2012) and marine controlled source electromagnetic data (Ray and Key, 2012).

Our paper describes our trans-dimensional inversion algorithm, the required input data and settings, the resultant uncertainty information and how to access the open source code. In principal the method can be applied to any range of frequencies, however we consider audio-frequency magnetotelluric (AMT) data because of its particular relevance to cover thickness estimation. Our algorithm is demonstrated with synthetic and real AMT data. The synthetic example demonstrates the extent of uncertainty information that can be gleaned from the method. The real example shows how the method has been successfully used to estimate cover thickness to within ten percent.

## METHOD AND RESULTS

### Inversion Algorithm

Our inversion program, which we call *rjmcmt*, is built upon an open-source library, developed at the Research School of Earth Sciences, Australian National University, called *rj-McMC* Hawkins (2013). The *C* library provides low-level routines for running reversible jump Monte-Carlo Markov chains for 1D and 2D spatial regression problems and also allows generalization to any spatial 1D and 2D problem through a user supplied data misfit function. Specifically, our program makes use of the library's 1D forward model functionality through the sampling routine *MPI\_part1d\_forwardmodel*.

Our program uses a 1D forward model function that generates magnetotelluric data, at a specified list of frequencies, for an isotropic layered resistivity model. The program has options to invert data in the form of either real and imaginary impedance, or apparent resistivity and phase, directly from Electrical Data Interchange (EDI) format files. When inverting impedance data we use the determinant of the impedance tensor ( $z = \sqrt{z_{xx}z_{yy} - z_{xy}z_{yx}}$ ). When inverting apparent resistivity and phase data, we use the geometric mean of the apparent resistivity ( $\rho = \sqrt{\rho_{xy}\rho_{yx}}$ ) and the arithmetic mean of the apparent phase ( $\theta = [\theta_{xy} + \theta_{yx}]/2$ ).

Relative and absolute noise standard deviation estimates for the data to be inverted are specified and combined (assuming independence) to generate the total noise estimate that is used in the inversion to calculate the error normalized (*L2-norm*) data misfit.

The user specifies the maximum number of layers allowed in the resistivity model, and the maximum allowed depth of the layer interfaces. The algorithm assumes uniform prior probability for the number of layers in the model and a log-uniform prior on the depths of the layer interfaces. The latter is because in the model depth is parameterized in terms of log-depth. The user also specifies a minimum and maximum resistivity range that is allowed, and the prior probability is assumed log-uniform over this interval, again this is because resistivity is parameterized in terms of log-resistivity.

The number of samples (models) for the burn-in period of the Markov chain is specified, which allows the data misfit to converge to an acceptable level before any samples are accepted into the ensemble. The total number of samples for each chain is also specified by the user. Since, the program is parallelized using the Message Passing Interface (MPI) paradigm, multiple Markov chains can be set running in parallel on a cluster computer or multi-core workstation, and the generated samples are transparently combined into a single ensemble.

The sampling routine (*MPI\_part1d\_forwardmodel*) is set running on all chains. Each chain is initialised with a model randomly drawn from the prior distribution. As the chain samples new models the algorithm is allowed to make one of four types of perturbations to the current model: (a) change the resistivity of a layer (*value-change*); (b) move an interface up or down (*move*); (c) create a new interface (*birth*); or (d) remove an interface (*death*). The new model is proposed by drawing random perturbations from a Gaussian proposal distribution. The proposed model is either accepted or rejected from inclusion onto the end of the chain based on an acceptance criterion ratio.

The acceptance criterion ratio is theoretically derived such that the Markov chain will eventually converge to an ensemble that is a good approximation of the posterior probability density (PPD) of the model given the data for the supplied noise estimates. Details of the derivation of the acceptance ratio are given in (Bodin *et al.*, 2012).

For the value-change and move propositions, the sampling algorithm favours accepting models with high likelihoods (low data misfits) and high prior likelihoods. For the birth and death propositions the acceptance probability is also a balance between the proposal probability, which encourages resistivity changes between adjacent layers, and the difference in data misfit, which penalizes resistivity changes if they degrade data fit. Also, given similar data fits, a proposed model has more chance of being accepted if the proposed model has fewer layers than the current model. This gives the algorithm a form of natural parsimony (Malinverno, 2002; Bodin and Sambridge, 2009).

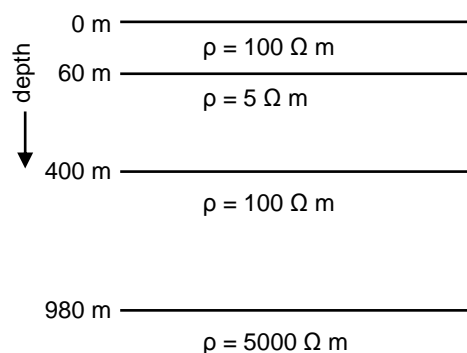
During the sampling, after the burn-in period, new models are added into a discretized 2D PPD posterior probability histogram. That is, for each discrete histogram depth-bin, the model resistivity is determined and the corresponding histogram resistivity-bin count is incremented. This progressively builds up an image representation of the desired posterior

probability. Similarly, a 1D changepoint histogram is built up by incrementing all depth-bins of the 1D histogram in which a layer interface falls.

At the conclusion of the sampling the 2D PPD histograms and the changepoint histograms from the parallel chains are merged. Several statistics are then extracted from the histograms including the mean, mode, 10th, 50th (median), and 90th percentile log-resistivity values in each depth-bin. Also the single most probable (highest likelihood) and lowest misfit models from all chains are saved. It is the distance or spread between the 10th and 90th percentile models that we may use to make assessments about model uncertainty - the narrower the spread the lower the uncertainty. The 1D changepoint histogram gives us insight into where the layer interfaces are most likely to occur.

### Synthetic Data Example

In this and the following section we present results from testing the *rjmcmt* program on synthetic and real data. All examples were run on 128 parallel MPI chains using the high-performance cluster computer hosted by the National Computational Infrastructure (NCI). For the synthetic example we constructed the four-layer 1D resistivity model shown in **Error! Reference source not found.** The model is a proxy for a for cover thickness estimation in some regions of Australia.



The top layer represents moderately conductive unsaturated near-surface transported regolith. The second layer represents highly conductive regolith material, typically saline or highly weathered clay rich sedimentary rocks. The third layer represents moderately conductive partially weathered rocks. The bottom layer represents resistive unweathered igneous and metamorphic crystalline basement rocks.

Synthetic data, in the form of apparent resistivity and phase, were generated at 40 frequencies over the AMT frequency band of 1 Hz to 10 kHz by forward modelling of the synthetic resistivity model shown in **Error! Reference source not found.** We added simulated Gaussian noise, which for apparent resistivity consisted of 5% relative error and absolute error of 0.01  $\Omega$  m, and for apparent phase data consisted of 2% relative noise and absolute error of 0.5 $^\circ$ .

**Figure 1: Four layered synthetic resistivity model used in the synthetic data inversion example.**

We then inverted the synthetic data using our *rjmcmt* program using 128 independent Markov chains in parallel. In the inversion we assigned data error estimates consistent with the simulated values above (i.e., 5%, 0.01  $\Omega$  m, 2% and 0.5 $^\circ$ ). All chains had a burn-in of 10,000 samples and length of 1 million samples, resulting in 128 million samples in total. We set the maximum number of layers to 20, the maximum allowable depth for layer interfaces to be 4000 m, and the allowable range of layer resistivities to be 0.1 to 100,000  $\Omega$  m respectively.

**Error! Reference source not found.** summarizes the results of the inversion of the synthetic data. **Error! Reference source not found.a** and **Error! Reference source not found.b** show the synthetic apparent resistivity and phase data, with their assigned error bars, and the predicted data from the forward model of the best fitting model in each of the 128 Markov chains (which happen to plot almost exactly on top of one another). There is nothing particularly enlightening about the best fitting model in each chain, but they are simply plotted to show that they fit the data.

**Error! Reference source not found.c** shows the convergence history of each Markov chain (blue traces). The vertical black line shows the end of the burn-in period at 10,000 samples, before which the chains are converging from high data misfits down to the expected data misfit of 80 (i.e., the total number of data) represented by the horizontal line. After the burn-in the chains remain fitting the data at close to the expected value, indicating that they are neither under or overfitting the data.

**Error! Reference source not found.d** shows the histogram of the number of layers in the models collected into the ensemble. It indicates that one or two layers cannot satisfactorily fit the data, and that a three layer model is the most likely. Four layers, the true number of layers, are also highly likely, but not as likely as three layers. For more than four layers the likelihood rapidly tails off.

**Error! Reference source not found.e** shows the log of the PPD histogram in pseudo-coloured shading. The higher probability areas of model space have the hotter (red) shading, and white areas have practically zero probability. Plotted on top of the shading is the true synthetic model (magenta). Also plotted are various summary models that have been extracted from the PPD histogram, specifically: the median or 50th percentile model (black); the 10th and 90th percentile models (black dashed); the mean model (blue); and the mode model (green). **Figure 3** shows slices through the PPD histogram at four different depths to provide extra insight and detail.

The PPD indicates that, as expected, the very conductive second layer is well resolved because there is a small spread between the 10th and 90th percentiles and the very sharp histogram slice through the 200 m depth-bin (**Figure 3**). The more resistive top layer is also well resolved, but there is some possibility of a higher resistivity than the true (synthetic) value.

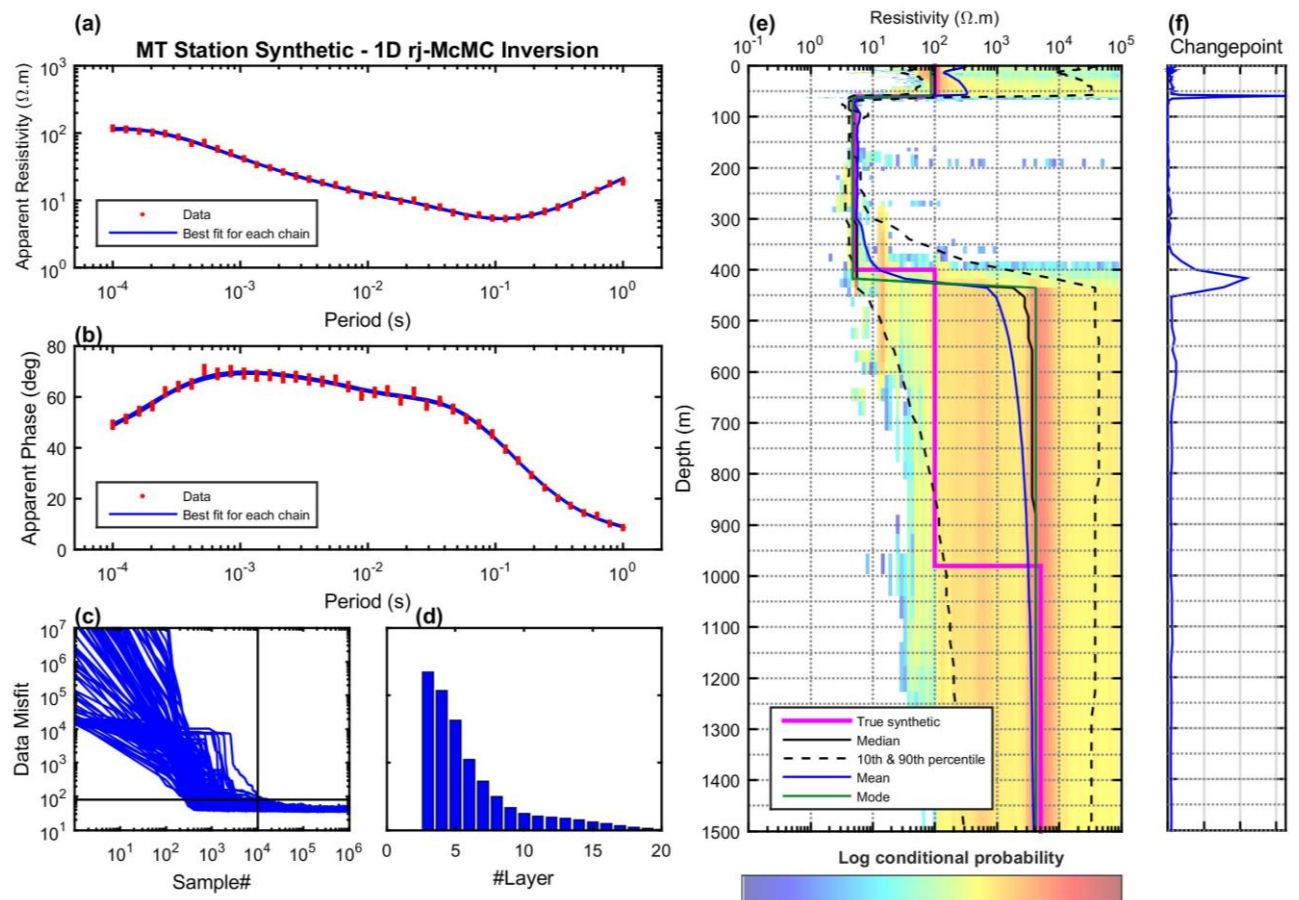


**Figure 2:** Plot summarising the results of the synthetic inversion, showing: (a) & (b) apparent resistivity and phase data and error bars (red) and the best fitting model from each Markov chain (blue); (c) data misfit convergence history for each Markov chain; (d) histogram of the number of model layers; (e) the true synthetic model, with the summary median, 10th and 90th percentile, mean and mode models over lying the pseudo-coloured shaded image of the 2D log-PPD histogram; and (f) the changepoint histogram showing the probability of where layers interfaces occur.

The 500 m PPD slice on **Figure 3** shows that there is a quite small indication of a resistivity equalling the true layer three resistivity value (100  $\Omega.m$ ) at that depth. However it shows that the resistivity of the fourth layer (5000  $\Omega.m$ ) is actually favoured much more. The PPD shows that this is the case throughout the range of the third layer (400 m to 980 m). In the fourth layer, at 1200 m depth the maximum probability is more or less aligned with the true resistivity (5000  $\Omega.m$ ), however there is still some possibility of resistivities as low as 100  $\Omega.m$ .

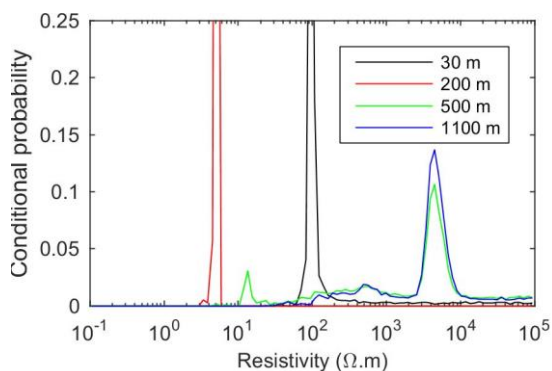


**Figure 3:** Slices through the synthetic inversion's PPD histogram at four different depths. Note the y-axis is clipped at 0.25 to allow extra detail to be shown.

This is a good demonstration of how the inversion of the synthetic data has not been able to clearly resolve the third and fourth more resistive layers into two separate layers. The parsimonious nature of the rj-McMC algorithm has preferred the simpler three layer models, which still adequately fit the data within the assigned noise levels. Only the addition of independent constraining information could resolve this non-uniqueness.

Figure 2f is the 1D changepoint histogram that shows the probability of a layer interface occurring within a particular depth-bin. The large narrow peak at ~60m shows that the bottom of the first interface has been resolved accurately and with low uncertainty. The other peak occurs at ~415 m, just below the

interface between the second and third layers in the true model (400 m). This peak is broader, as would be expected, because of the diminishing sensitivity to interface position with depth. Interestingly this second layer interface was resolved quite well even though the resistivities of the third and fourth layers were indistinguishable. The interface between the third and fourth layers at 980 m was not resolved at all.

### Real Data Example

The real data example is from AMT data collected in the Southern Thomson Orogen located in northern New South Wales and southern Queensland. Basement geology in this region is characterised as Palaeozoic rocks that underlie the Jurassic to Cretaceous Eromanga Basin sequences (Roach *et al.*, 2015). The data were acquired to estimate cover thickness prior to a drilling programme and thereby reduce the uncertainty and risk associated with intersecting the targeted stratigraphy.

We selected AMT data from a station at the proposed borehole site called Adventure Way (AMT Station Adv1) for the example. We inverted real and imaginary components of the impedance tensor determinant for 51 frequencies in the range of 1 kHz to 10 kHz. On both components we assessed the data errors to be 5% relative noise and 0.025 mV/km/nT noise floor. We ran the inversion using the exact same settings as in the synthetic example above (i.e., 128 chains, 10,000 burn-in samples, 1 million samples, 20 layers maximum, 4000 m maximum interface depth, and 0.1 to 100,000  $\Omega$  m resistivity range).

A summary of the results are given in Figure 4 in the same fashion as for the synthetic example in Figure 2, except this time we have added the stratigraphy log from the Adventure Way borehole in Figure 4g. The results in Figure 4a-c show that the data were fitted successfully well before the burn-in. Figure 4d indicates that a 5 or 6 layer model is the most likely.

The 2D log-PPD histogram shading and the summary models in Figure 4e suggests a high likelihood of a very conductive zone in the top 50 m that corresponds well with the Winton Formation (0-48 m) as shown on the borehole stratigraphy log Figure 4g. There is also an indication of the existence of the interface between the Winton and Wallumbilla Formations at 45-50 m on the 1D changepoint histogram (Figure 4f).

The inversion suggests that the profile remains conductive, with some possibility of resistive zones, until approximately 250 m where a significant transition from conductive to resistive material occurs. The broad peak of the transition in the changepoint histogram between 225-275 m coincides with the Wyandra Sandstone Member Aquifer or Cadna-owie Formation. Below 275 m the inversion profile is definitively resistive and is within 10% of where the crystalline basement greenschist begins at 300 m depth.

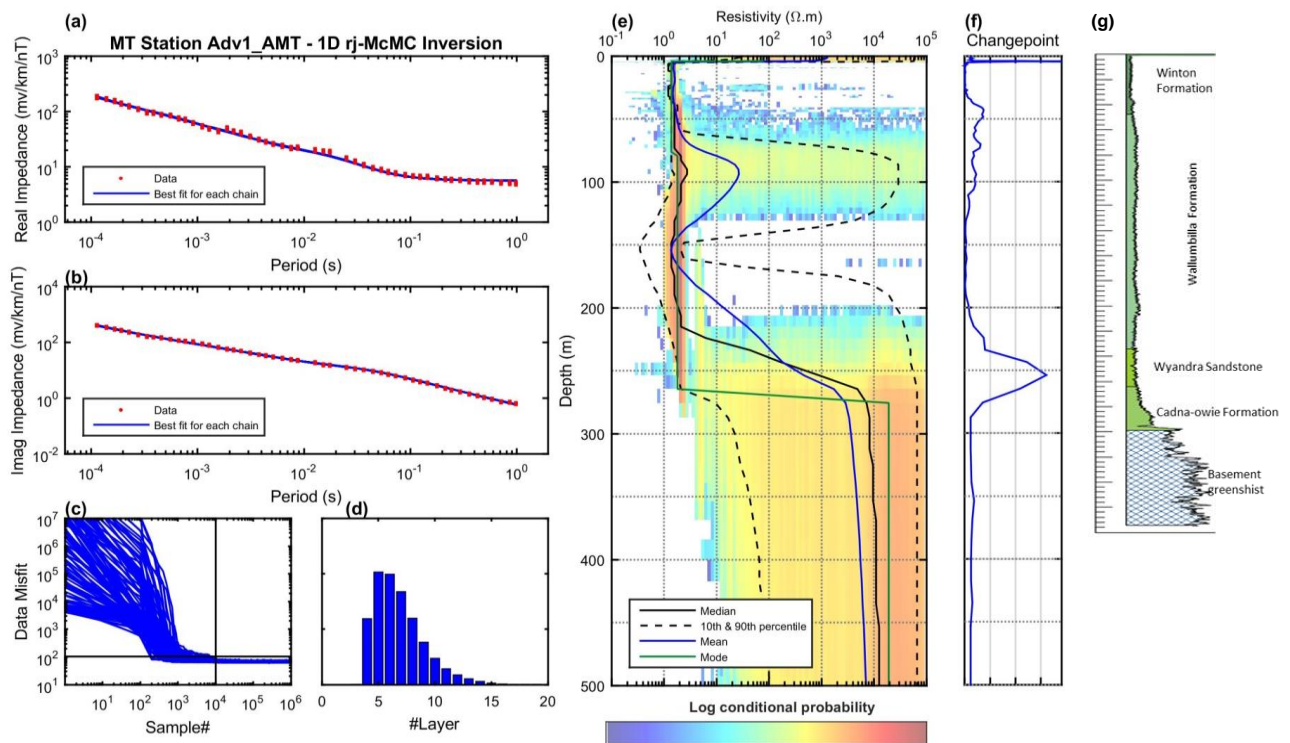


**Figure 4:** Plot summarising the results of the real data inversion example: (a) & (b) real and imaginary impedances and error bars (red) and the best fitting model from each Markov chain (blue); (c) data misfit convergence history

for each Markov chain; (d) histogram of the number of model layers; (e) the summary median, 10th and 90th percentile, mean and mode models over lying the pseudo-coloured shaded image of the 2D log-PPD histogram; (f) the changepoint histogram showing the probability of where layers interfaces occur; and (g) the stratigraphy log from the adjacent borehole.

## OPEN SOURCE CODE

The software is accessible as C++ source code and as executables for 64 bit Windows® PCs. The source code is packaged in a Git code repository and may be downloaded from Geoscience Australia's GitHub® repository <https://github.com/GeoscienceAustralia/rjmcmt>. The code can be compiled using most modern C++ compilers on both Linux and Windows® based systems. The code is fully parallelized for execution on a high performance cluster computer or on a multi-core shared memory workstation via MPI. In due course we also expect to make the algorithm available as a service on the Australian National Virtual Geophysics Laboratory (ANVGL) portal (<http://www.anvgl.ga.gov.au>).

The source code and binaries are released under the GNU GPL Version 2.0 Licence, making it available for anyone to use at no cost, including for academic, government and commercial purposes. All of the programs are command line driven and hence do not have graphical user interfaces. The code will be accompanied by basic user documentation and examples. However, Geoscience Australia will not be providing user support for the source code installation and/or program usage.

## CONCLUSIONS

The program that we have developed for 1D probabilistic inversion of magnetotelluric data is fully parallelized and has been made available in open-source form. The program can invert complex impedance tensor data, as well as derived apparent resistivity/phase data in EDI file format.

It provides a wealth of information from the inversion of each station. This includes the a histogram of the probable conductivity-depth distribution, plus mean, mode, median and 10th and 90th percentile summary models, and a histogram of the probable interfaces depths. The algorithm provides more robust estimates of uncertainty than the traditional linearized deterministic methods.

The synthetic example demonstrates the degree to which the resulting probabilistic information can be interpreted. It also nicely demonstrated the limitation of geophysical data due to non-uniqueness. The real data example demonstrates how the method can be applied to cover thickness estimation and that the results compare favourably with borehole stratigraphy logs. An appealing feature of the method is the ability to pick the position of layer interfaces directly from the changepoint histogram. This allows a more straightforward and repeatable interpretation of cover thickness, and associated uncertainty, than is possible from regularized smooth model inversions. The method will be a valuable addition to a range of other cover thickness estimate tools.

## ACKNOWLEDGMENTS

We thank Professor Malcolm Sambridge and Dr Rhys Hawkins from the Research School of Earth Sciences, Australian National University, for their advice on the method and assistance with their open-source *rj-McMC* library on iEarth. This abstract is published with the permission of the CEO, Geoscience Australia.

## REFERENCES

- Bodin, T. and Sambridge, M., 2009. Seismic tomography with the reversible jump algorithm. *Geophysical Journal International* **178**(3), 1411-1436.
- Bodin, T., Sambridge, M., Tkalčić, H., Arroucau, P., Gallagher, K. and Rawlinson, N., 2012. Transdimensional inversion of receiver functions and surface wave dispersion. *Journal of Geophysical Research* **117**(B02301). doi: 10.1029/2011JB008560.
- Brodie, R. C. and Sambridge, M., 2012. Transdimensional Monte Carlo inversion of AEM data. *ASEG Extended Abstracts* **2012**(1), 4.
- Constable, S. C., Parker, R. L. and Constable, C. G., 1987. Occam's inversion; a practical algorithm for generating smooth models from electromagnetic sounding data. *Geophysics* **52**(3), 289-300.
- Hawkins, R., 2013. iEarth web page for rj-McMC. Online: <http://www.earth.org.au/codes/rj-McMC>.
- Malinverno, A., 2002. Parsimonious Bayesian Markov chain Monte Carlo inversion in a nonlinear geophysical problem. *Geophysical Journal International* **151**(3), 675-688.

Minsley, B. J., 2011. A trans-dimensional Bayesian Markov chain Monte Carlo algorithm for model assessment using frequency-domain electromagnetic data. *Geophysical Journal International* **187**(1), 252-272.

Ray, A. and Key, K., 2012. Bayesian inversion of marine CSEM data with a trans-dimensional self parametrizing algorithm. *Geophysical Journal International* **191**(3), 1135-1151. doi: 10.1111/j.1365-246X.2012.05677.x.

Roach, I. C., McPherson, A. A., Clarke, J. D. A., Brodie, R. C., Doublier, M. P., Armistead, S. E., Skirrow, R. G. and Main, P. T. (ed), 2015. Southern Thomson Orogen VTEMplus AEM Survey: Using airborne electromagnetics as an UNCOVER application. Geoscience Australia. **Record 2015/29**. Online: [https://d28rz98at9flks.cloudfront.net/83844/Rec2015\\_029.pdf](https://d28rz98at9flks.cloudfront.net/83844/Rec2015_029.pdf).